A Semi-stochastic Numerical Model of Adult Hippocampal Neurogenesis

Pınar Öz

Üskudar University, Faculty of Engineering and Natural Sciences, Department of Molecular Biology and Genetics,
34362, Istanbul, Turkey
(ORCID: https://orcid.org/0000-0001-6006-9921)

Abstract: Adult neurogenesis in dentate gyrus (DG) is a prominent contributor in the dynamics of hippocampal memory networks. This discrete model aims to estimate the temporal changes in the neural progenitor cell (NPC) populations in DG, together with the products of differentiation – immature neurons, astrocytes and oligodendrocytes. The dynamics are described in an ideal environment, where there is no limit for the total volume and all required chemical and physical cues that direct neurogenesis are continuously available. The system works independently on three levels. Each level is defined as the dynamics in a stage of neurogenesis with three types of NPCs: type I cell (radial glia), type II cell (transiently amplifying cells) and type III cell (neuroblasts). Cell fate was introduced as a semi-stochastic process (a choice) with a population limit for each cell type. Although it is based on discrete processes and has a rather simplistic approach, the simulations successfully provide a numerical template for adult neurogenesis, which can be further modified and implemented in a hippocampal trisynaptic loop network.

Yetişkin Hipokampal Nörogenezinin Yarı-stokastik Nümerik Bir Modeli

Özet: Dentat girusta (DG) görülen yetişkin nörogenezinin hipokampal bellek ağlarındaki işleve önemli bir katkı sunduğu kabul edilmektedir. Sunulan ayrık sayısal model DG'de bulunan nöral progenitör hücre (NPH) popülasyonlarında ve bu süreçlerin ürünlerindeki (immatür nöron, astrosit ve oligodendrosit popülasyonları) temporal değişimleri modellemeyi amaçlamaktadır. Süreçler toplam hacimde bir limitin olmadığı ve nörogenezi yönlendiren tüm kimyasal ve fiziksel düzenleyicilerin devamlı ulaşılabilir olduğu ideal bir ortamda tanımlanmıştır. Sistem üç temel seviyede bağımsız olarak çalışmaktadır. Her seviye nörogenez süreçlerindeki bir aşama olarak tanımlanmıştır ve popülasyonlar üç temel hücre tipinden oluşmaktadır: Tip I (radyal glia), tip II (geçici çoğalan hücre) ve tip III (nöroblast). Hücre kaderi, her hücre tipi için bir popülasyon limiti olan yarı-stokastik bir süreç (bir seçim) olarak sisteme eklenmiştir. Sunulan model, ayrık süreçlere dayanmasına ve basitleştirilmiş bir yaklaşım izlemesine rağmen, yetişkin nörogenezinin sayısal bir taslağını başarılı şekilde üretmektedir ve farklı modülasyonlarla bir hipokampal trisinaptik devre ağına yerleştirilebilir.

1. Introduction

In the adult mammalian brain, neurogenesis continues to occur in well-identified neurogenic niches, i.e. the subventricular zone (SVZ) on the walls of lateral ventricle and the subgranular zone (SGZ) of dentate gyrus (DG) in hippocampus [1], [2],[3],[4],[5].

In SGZ, three main types of neural precursor cells (NPCs) are identified. The radial-glia-like cells (Type I cells) carry astrocytic properties, such as the expression of glial fibrillary acidic protein (GFAP) [6]. In the adult brain, Type I cells constitute a largely quiescent cell population that only occassionally divide [7],[8]. However, when triggered, these cells can proliferate through symmetric or asymmetric cell division [3],[9],[10]. It is suggested that Type I cells can possess different morphologies and behaviors, and that it is possible for one Type I cell to generate an astrocyte while another one can be on the track of neurogenesis [6]. Eventhough the literature on this difference is still not sufficient, recent data suggest that there are indeed distinct subclasses of Type I cells [6], [11], [12], [13].

Asymmetric cell division of a Type I cell is suggested to produce the second type of NPCs in this region - the

transiently amplifying cells (Type II) [1], [6], [14], [15]. Type II cells are transient in nature, due to the fact that they can divide very rapidly, however, with much lower self-renewal capacity compared to Type I cells. Through these divisions they can either produce identical Type II cells or differentiate into neuroblasts [1],[4],[5],[14],[15].

Type II cells typically consist of two subclasses, Type IIa and Type IIb, which differ in the expression of biomarkers and also in behavior [8],[16],[17]. Type IIa typically share common glial properties with Type I cells and they are highly proliferative. Type IIb is more lineage-determined progeny of Type IIa. They,in turn, give rise to neuroblasts (Type III cells) [3], which possess less self-renewal capacity. Neuroblasts are unipotent, meaning a determined cell fate towards producing new neurons [1],[5],[6].

Throughout these stages of neurogenesis, gliogenesis follows also in parallel and both processes can stem from adult NPCs [18]. The interplay between neurogenesis and gliogenesis is known to be affected by various factors, such as bone morphogenic protein (BMP), fibroblast growth factor (FGF), epidermal growth factor (EGF) and sonic hedgehog (Shh) [19],[20],[21],[22]. Astrocytes and oligodendrocytes are the two main types of glia that have a strong connection with the processes of neurogenesis and also with the maturation of newborn neurons. Astrocytes can be produced from NPCs via asymmetric cell division and can also be directed toward neurogenesis by forced expression of transcription factors, such as Pax6, or when inducing factors such as brain-derived neurotrophic factor (BDNF) are supplied [23],[24],[25],[26]. Interestingly, the NPCs in SVZ can be triggered to produce either neurons or oligodendrocytes, where the choice seems to depend on the platelet-derived growth factor-α (PDGFα) receptor signaling [27]. It is not entirely known whether glial cells can be generated from adult NPCs *in vivo*, however, the information on the interplay between neurogenesis and gliogenesis strongly suggest that they can be observed at least as *side-products* of neurogenesis in neurogenic niches.

The hippocampal adult neurogenesis (HANG) model aims to provide a rather numerical tool that can be implemented in the trisynaptic loop network models of hippocampus. Developing a theoretical framework for the HANG can be used to predict the neurogenic processes and the outcomes of its regulation. Then, the framework can be implemented in a larger network model to provide information on the newborn neuron numbers and how their addition regulates the network activity. In this study, a framework, that includes a semi-stochastic cell fate determining function, is developed to analyze the critical rates of various neurogenic processes and its capacity to produce the population growth patterns that can be compared to experimental data *in vivo* and *in vitro*.

2. Material and Method

2.1. The Numerical Model for Subgranular Zone Adult Neurogenesis

The HANG model was implemented in Matlab v.2016b and consists of three main stages : Type I cell dynamics, Type II cell dynamics and Type III cell (neuroblast) dynamics. Newborn astrocytes are produced from Type I and Type II cells, while oligodendrocytes and newborn (immature) neurons are produced from the third stage only. In all three stages, the choice of cell fate is randomized and implemented with the function δ. The model is summarized in Figure 1 and explained in the following sections.

2.1.1. Choice of Cell Fate

The molecular mechanisms in the cell that lead to either proliferation, differentiation or apoptosis are implemented in the model by a simple randomized cell fate function, represented by δ (Figure 1). When the cell matures, the intracellular and extracellular cues will direct the cell to either proliferate, differentiate or die. From a simplistic approach, apoptosis is not included in the fate choices, and a constant ratio of cells are assumed to die in a given duration Δt. Environmental cues driving the probability of differentiation (p_d) or proliferation (p_p) at three stages of HANG model are represented in δ as the ratio of population that are directed to that fate. When δ is not implemented, it can be assumed that a constant ratio of the cell population proliferates where the rest differentiates. When δ is implemented, however, this process is randomized, with a boundary condition where there is an average ratio of cells ($\bar{p}$) that are expected to follow a specific fate.

This process is represented with the function δ as in equations 1 and 2,

$$\delta(\bar{p}, N) = \sum_{i=1}^{N} u_i(x, \bar{p}) \qquad (1)$$

$$u_i(x, \bar{p}) = \begin{cases} 0 & , \quad x \geq \bar{p} \\ 1 & , \quad x < \bar{p} \end{cases} \qquad (2)$$

where x is a random number between 0 and 1 representing the combination of intracellular triggers and environmental cues driving the cell to specified fate and N is the number of cells in the population.

2.1.2. Type I cell dynamics

Type I cells of HANG model are assumed to either proliferate or differentiate. Type I cell proliferation can be through symmetric cell division, producing two Type I cells, or asymmetric cell division, producing an astrocyte and a Type I cell. It is assumed that :
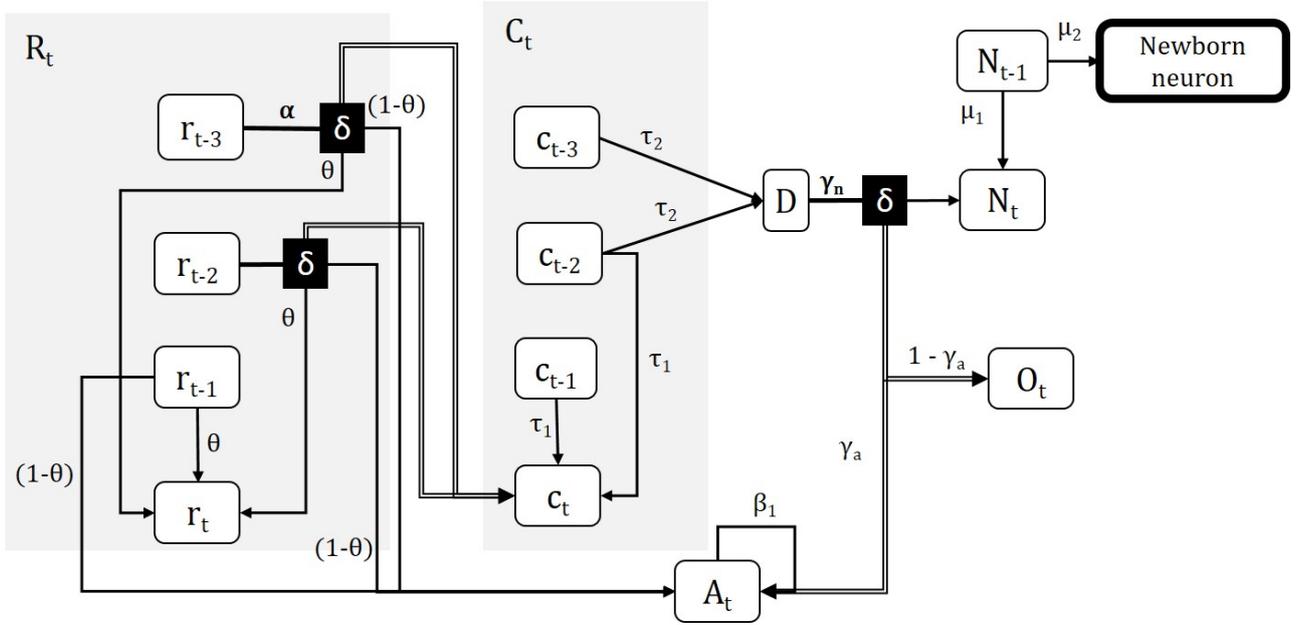
Figure 1. The general outline of HANG model. Details of the model design, processes and rates are given in the text. r: Type I cell, c: Type II cell, D:differentiating Type II cell, N: neuroblast, A: astrocyte, O:oligodendrocyte.

1. Newborn Type I cells are required to mature before either proliferation or differentiation.

2. Proliferation occurs either through symmetric or asymmetric cell division. Mature cell can produce a daughter cell through symmetric cell division with the probability θ, or it can produce an astrocyte through asymmetric cell division with the probability 1- θ.

3. Once divided the Type I cell can then proliferate once more or differentiate into a Type II cell. The choice is decided via δ with the average ratio of cell population that choose to proliferate ($\bar{p}_p^r = \alpha$). If a cell chooses to proliferate, it will go through the process as described before.

4. A cell is assumed to die after its second proliferation.

The described dynamics of Type I cell population (R) at time t is then formulated over three generations of Type I cells (r) as below.

$$r_t = \theta(r_{t-1} + \delta(\alpha, r_{t-2})) \quad (3)$$

$$R_t = \sum_{i=t-2}^{t} r_i \quad (4)$$

The number of astrocytes that are produced from Type I cells (A_t) at a time point t is

$$A_{r,t} = (1-\theta)(r_{t-1} + \delta(\alpha, r_{t-2})), \quad (5)$$

and the number of differentiated Type I cells (c_t) at t is

$$c_{r,t} = r_{t-2} - \delta(\alpha, r_{t-2}). \quad (6)$$

2.1.3. Type II cell dynamics

Type II cells, or transiently amplifying cells, are a transition stage from progenitor radial glia to neuroblasts; they quickly proliferate or differentiate, however, for a short duration of time and under heavy stress of cell death [1],[2],[8],[28]. A portion of the newborn Type II cells are differentiated from Type I cells ($c_{r,t}$), however, differentiating astrocytes ($c_{a,t}$) and proliferating mature Type II cells can also produce newborn Type II cells. It is assumed that :

1. Only a portion of newborn Type II cells ($\tau_1 . c_{t-1}$)survive and proliferate.

2. A portion of once divided Type II cells ($\tau_2 c_{t-2}$) differentiate, while a portion of the rest proliferate again ($\tau_1(1-\tau_2)c_{t-2}$). The remaining portion of the population dies.

3. A portion of twice-divided Type II cells ($\tau_2 c_{t-3}$) differentiate and the rest dies.

Therefore, the number of newborn Type II cells (c_t) an the total number of cells in the Type II cell population (C_t) at a given time t can be expressed as below.

$$c_{\alpha,t} = \beta_1 A_{t-1} \quad (7)$$
$$c_t = c_{r,t} + c_{\alpha,t} + \tau_1 c_{t-1} + \tau_1^2(1-\tau_2)c_{t-2} \quad (8)$$
$$C_t = c_t + \tau_1 c_{t-1} + \tau_1^2(1-\tau_2)c_{t-2} \quad (9)$$

Type II cells that are ready to differentiate can produce either Type III neuroblasts(N), astrocytes (A), or oligodendrocytes (O). The number of differentiating Type II cells at a given time t can be expressed as below.

$$D_t = \tau_1 \tau_2 c_{t-1} + \tau_2 c_{t-2} \quad (10)$$

2.1.4. Neuroblast dynamics

Type III cells, or neuroblasts, can be differentiated from Type II cells and can be produced via proliferation from mature neuroblasts.

$$N_t = \mu_1 N_{t-1} + \delta(\gamma_n, D_t) \qquad (11)$$

The mature neuroblasts that do not proliferate at a given time t can differentiate into young neurons $((1-\mu_1)\mu_2 N_{t-1})$ and the remaining population is assumed to die. The newborn neurons migrate to the *stratum granulosum* and get integrated into existing neural network [1],[2],[8]. At this stage, it is critical that the young neuron receives adequate glutamatergic and GABAergic inputs. The neurons that are not innervated adequately will not survive. The HANG model does not include the migration process of the young neuron and ends with obtaining the number of newborn neurons in the system.

2.1.5. Glia Populations

Astrocytes can be produced from Type I cells via asymmetrical cell division ($A_{r,t}$) or from differentiating Type II with an average ratio γ_a of Type II cells that did not differentiate into neuroblasts.

$$A_{D,t} = \gamma_\alpha (D_t - \delta(\gamma_n, D_t)) \qquad (12)$$

The mature astrocytes proliferate to form newborn astrocytes with a rate of β_1 and differentiate into Type II cells with a rate of β_2. The death rate for astrocytes are introduced as ϕ_a. Then, the total number of astrocytes in the system can be expressed as below.

$$A_t = A_{r,t} + A_{D,t} + (\beta_1 - \beta_2 - \phi_a)A_{t-1} \qquad (13)$$

The differentiating group of Type II cells, that did not produce neuroblasts or astrocytes, are assumed to differentiate into oligodendrocytes.

$$O_t = (1 - \gamma_\alpha)(D_t - \delta(\gamma_n, D_t)) \qquad (14)$$

2.2. Implementation of Aging

The impact of age on the proliferation and differentiation rates (x) were implemented on α, θ and τ_1, such that the rates start to exponentially decline as

$$x_t = x_0 e^{-\lambda t} \qquad (15)$$

when Type I cell population reaches to a critical value (r_{max}) and continues to decline with the same rate until the organism is 90 days old. After this age, the rate declines with the rate λ_2, where $\lambda_2 < \lambda_1/2$. For all simulations, $r_{max} = 7.5x10^3 r_0$ for α, $r_{max} = 10^3 r_0$ for θ and $r_{max} = 2x10^3 r_0$ for τ_1. The rates λ_1 and λ_2 were determined over

previously reported immunohistochemistry data from mice and rats [29], [30],[31].

2.3. Parametric Analysis

For parametric analysis, Δt was 1 day and the simulation was run for 30-days over 20 repetitions. The default values for the parameters were α=0.6, θ = 0.8, β_1 = 0.5, β_2 =0.2, τ_1 = 0.7, τ_2 = 0.5, γ_n = 0.7, γ_a = 0.8, μ_1 = 0.2, μ_2=0.3. The population mean and standard deviation for each day were estimated over repetitions. The impact of parameters such as α, β_2, γ_n, τ_1 and τ_2 were analyzed by varying the values in the ranges as given in Results. The number of cells at 30th day were plotted for each value in the range. The plots displaying the number of cells on 30th day vs the varying parameter were fit with the functions given in Results, using robust fitting with bisquare weights. Adjusted R-square (ARS) values are given as the means for goodness of the fit.

3. Results

3.1. Default Model

The HANG model was first initiated with the default parameters and the population growth was recorded over 50 repetitions for 60 days(Figure 2). First type II cells emerge after 5 days, whereas it takes at least 10 days for the differentiation of the first neuroblast. As astrocytes can be generated from all three stages, the first astrocyte emerges during the first three day of the simulation. Oligodendrocytes emerge around $20^t h$ day, as the generation of oligodendrocytes occur only at the third stage. Around $20^t h$ day, first immature neurons appear in the system as well and each day the number of new immature neurons increase, which correlates with the increasing number of neuroblasts. On 60th day, the ratio of Type I cells in the resulting cell population was 43.7% $\pm$ 6.9, Type II cells 36.7% $\pm$ 5.8, neuroblasts 11.4% $\pm$ 1.8, astrocytes 4.4% $\pm$ 0.7, oligodendrocytes 1.8% $\pm$ 0.3 and new neurons 1.9% $\pm$ 0.3 (Figure 3).
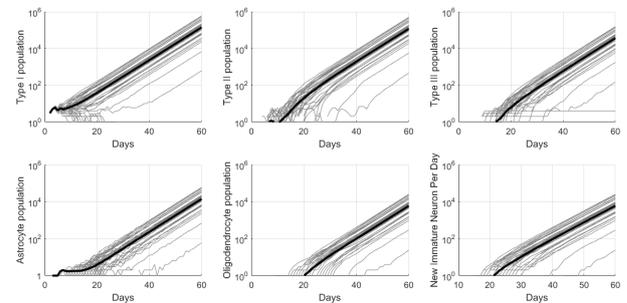
Figure 2. Cell populations with default parameters. The gray lines represent the population growth for each repetition. Black lines represent the average population growth.
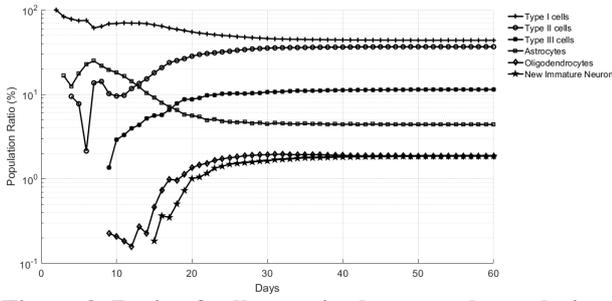
Figure 3. Ratio of cell types in the general population on 60th day. The number of each cell type on 60th day was normalized with the total number of cells in the system.

3.2. Parametric Analysis of HANG model

The critical rates of the model (α, θ, τ_1 and τ_2) were modified in a range from 0 to 1 to see the impact on the resulting populations of HANG model. The population ratios after day 30 remained almost constant for all cells of the defult model, therefore the impact of each parameter was analyzed over the number of cells on day 30 for each population. The initial number of Type I cells (r_0) was 10 for all trials.

3.2.1. The impact of α on cell populations

Since α controls the ratio of Type I cells that choose to proliferate and all the remaining cell populations depend on Type I cells as the primary source, it was expected to affect all of the resulting cell populations in the model, making it the one of the most critical parameters in the model. Figure 4 displays the result for the varied values of α in the range 0 to 1. As expected, the number of Type I cells on 30th day exponentially increase as α increased. For the Type I cells and astrocytes, the relation could be fitted with the exponential equation (ARS$_R$ = 0.999, ARS$_A$ = 0.999).

$$y = a_1 e^{a_2 x} \tag{16}$$
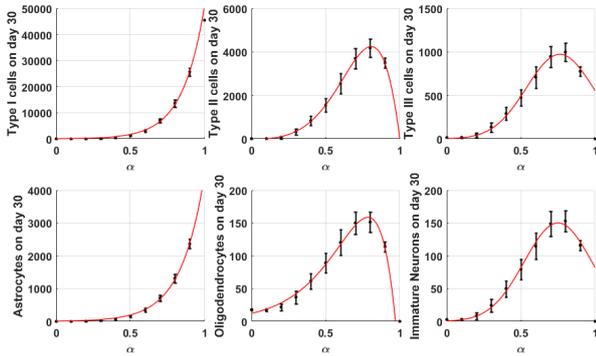
Figure 4. The impact of α on the population growth. The number of cells on day 30 for α between 0 and 1 was displayed for all cell types. The cell number was averaged over 100 trials, and error bars represent standard errors. Lines represent the fitted curves and the details of the fitting is explained in the text.

The relation between α and the number of cells on 30th day were fitted for the Type II cells with the equation 17 (ARS$_C$

= 0.999), whereas number of cells for neuroblasts and immature neurons were fitted with the equation 18 (ARS$_{TIII}$ = 0.943, ARS$_{Nr}$ = 0.944). The number of oligodendrocytes vs. α was best fitted with the equation 19 (ARS$_O$ = 0.983).

$$y = a_1 e^{\left(-\left(\frac{x-a_2}{a_3}\right)^2\right)} + a_4 e^{\left(-\left(\frac{x-a_5}{a_6}\right)^2\right)} \tag{17}$$

$$y = a_1 e^{\left(-\left(\frac{x-a_2}{a_3}\right)^2\right)} \tag{18}$$

$$y = a_1 e^{a_2 x} + a_3 e^{a_4 x} \tag{19}$$

For the type II cells, the number of cells on 30th day did not significantly change for $\alpha < 0.3$, increased between 0.3 and 0.8, and decreased for $\alpha > 0.8$. A similar pattern could be observed for neuroblasts : The number of cells on 30th day did not significantly change for $\alpha < 0.2$, increased between 0.2 and 0.8, and decreased for $\alpha > 0.8$. For both populations, a directly proportional increase in population size could only be observed for $\alpha \geq 0.8$. When α=1, both populations were exterminated. A similar pattern was also observed for oligodendrocyte population (Figure 4). Astrocyte population displayed a similar pattern of population growth with Type I cell population.

3.2.2. The impact of θ on cell populations

For all populations except neuroblasts, the population diminished until day 30 if $\theta < 0.5$. (Figure 5). When $\theta \geq 0.5$, the number of cells increased exponentially by increasing θ until reaching to a plateau at $\theta = 0.9$ For all cell types except astrocytes, the relation between cell number and θ could be represented with the equation 17 for $\theta \geq 0.5$. (ARS$_{TI}$ = 0.999, ARS$_{TII}$ = 0.999, ARS$_{TIII}$ = 0.999, ARS$_O$ = 0.999, ARS$_N$ = 0.999).

Astrocyte number - θ relation were fitted with the equation 20 (ARS=0.999).

$$y = a_1 e^{\left(-\left(\frac{x-a_2}{a_3}\right)^2\right)} + a_4 e^{\left(-\left(\frac{x-a_5}{a_6}\right)^2\right)} \tag{20}$$

3.2.3. The impact of τ_1 and τ_2 on cell populations

The increase in τ_1 (Figure6) and τ_2 (Figure 7) did not affect the Type I cell population. The sizes of other populations responded to the increase in τ_1 if $\tau_1 \geq 0.8$. The increase in τ_2 did not affect the astrocyte population. The amount of Type II cells decreased with increasing τ_2 until reaching to a plateau around $\tau_2 = 0.6$. The number of neuroblasts, oligodendrocytes and immature neurons increased until $\tau_2 < 0.4$, and reached to a limiting number after this value.

The population size response to τ_1 and τ_2 for populations except Type I cells could be represented with the equation 19 (ARS$_{TII}$ = 0.999, ARS$_{TIII}$ = 0.999, ARS$_A$ = 0.999, ARS$_O$ = 0.999, ARS$_N$ = 0.999).
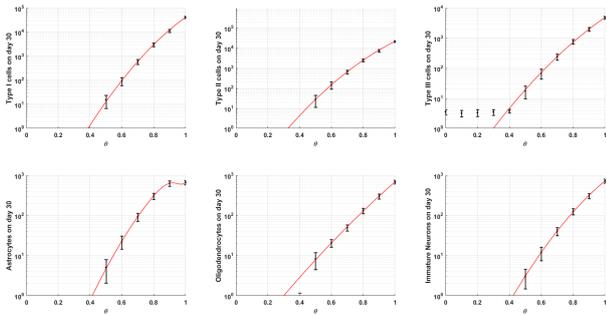
Figure 5. The impact of θ on the population growth. The number of cells on day 30 for θ between 0 and 1 was displayed for all cell types. The cell number was averaged over 100 trials, and error bars represent standard errors. Lines represent the fitted curves and the details of the fitting is explained in the text.
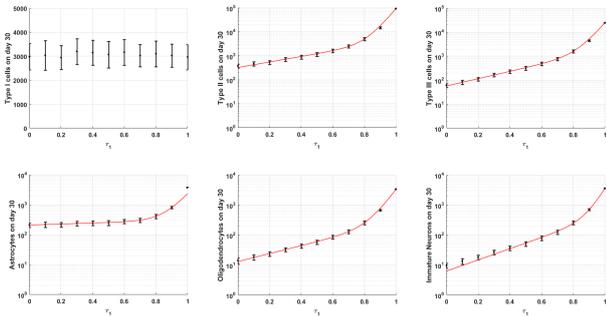
Figure 6. The impact of τ_1 on the population growth. The number of cells on day 30 for τ_1 between 0 and 1 was displayed for all cell types. The cell number was averaged over 100 trials, and error bars represent standard errors. Lines represent the fitted curves and the details of the fitting is explained in the text.

3.3. Simulation of Age-related Decrease in Proliferation Rates

The decrease in rates α, θ and τ_1 was implemented as described in Section 2.2, with $r_0 = 2500$, $\lambda_1 = 0.01$ and $\lambda_2 = 0.001$. Critical age was 90 days. The change in the population sizes for all cell types by age during a 7 month period was as shown in Figure 8. The peak population size was observed on 39th day for Type I cells, on 51st day for Type II cells, on 55th day for Type III cells, on 46th day for astrocytes and on 65th day for oligodendrocytes. The highest number of new immature neurons produced in this system was on 56th day. After the peaks, the population size decreased exponentially.

4. Discussion and Conclusion

The HANG model was designed to provide a numerical tool, to be later implemented in the trisynaptic loop network models of hippocampus. The focus was to develop a theoretical framework for the prediction of the neurogenic processes in adult mammalian hippocampus and the outcomes of its regulation. The HANG model differs from previous deterministic models [32],[33], [34],[35] by the types of cell populations included in the model, the implementation of maturation for NPCs and
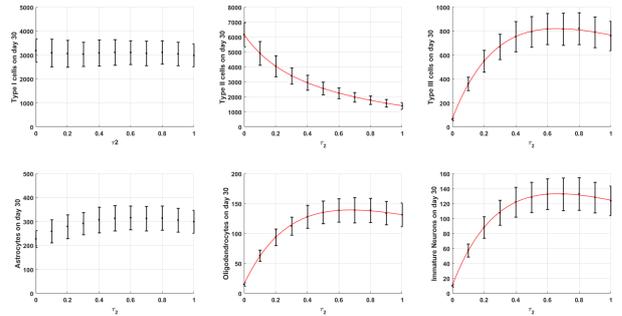
Figure 7. The impact of τ_2 on the population growth. The number of cells on day 30 for τ_2 between 0 and 1 was displayed for all cell types. The cell number was averaged over 100 trials, and error bars represent standard errors. Lines represent the fitted curves and the details of the fitting is explained in the text.
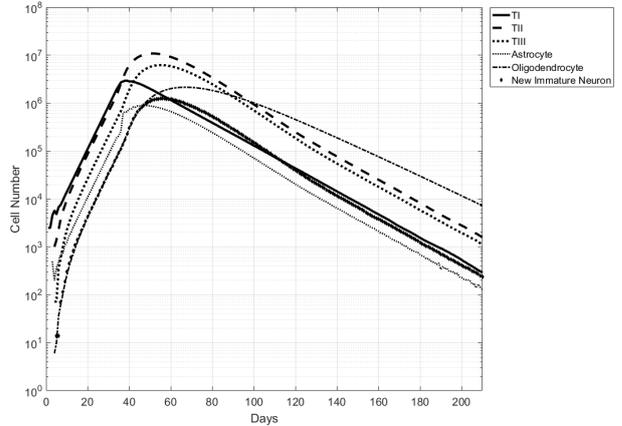
Figure 8. The impact of age-related decline in proliferation rates on the population growth. $r_0 = 2500$, $\lambda_1 = 0.01$, $\lambda_2 = 0.001$, critical age = 90 days

by the implementation of a semi-stochastic *choice of fate* function that acts as a simplified rule to mimic the non-deterministic cellular and environmental factors that drives the cell fate.

The molecular mechanisms that lead to either proliferation, differentiation or apoptosis of the cell was implemented as a semi-stochastic *choice of fate* function in HANG model, which produced a dynamic effect in these processes and in the resulting population sizes mimicing what could be observed under physiological conditions. Eventhough this function presents an extremely simplified rule, it was enough to produce the variations in population sizes that could represent the deviations in experimental measurements from trial to trial. In this setting, no physical limitations, such as limited space or nutrients, were introduced. Therefore, the logarithmic growth observed in the results could be expected under these conditions.

Parametric analyses explored the effect of critical rates such as α, θ, τ_1 and τ_2 on resulting population sizes. Among these, the variations in α was expected to affect all populations, as it directly manipulates the size and the fate of Type I cell population, which acts as the primary

source for the production of other cell types. Type II cells and neuroblasts depend on the number of Type I cells that choose to differentiate. Therefore, increasing the ratio of proliferating cells can be expected to decrease their numbers. It should be noted, however, that due to increased number of Type I cells, there are still plenty of cells that differentiate, which continues to feed the populations of Type II and Type III, and the effect of choice towards proliferation showed itself only after $\alpha=0.8$. When $\alpha=1$, none of the cells differentiate into Type II and Type III, which leads to the extermination of both cell populations. Astrocytes are generated from Type I and Type II, therefore an increase in the cell number of any of these populations can be expected to increase the number of astrocytes, when θ and γ_a are kept constant. The result (Figure 4) indicates a stronger impact of Type I cell proliferation on the number of astrocytes on day 30 compared to neuroblasts, which could also be expected as there is more than 10-fold Type I cells compared to neuroblasts. Oligodendrocytes are only generated from neuroblasts, therefore it was expected that their relation with α follows neuroblast pattern. As shown in Figure 4, the pattern was the same with neuroblasts. The number of new immature neurons generated on day 30 also followed the pattern of neuroblasts, as these cells could only be differentiated from them.

The rate θ determines the ratio of symmetrically dividing Type I cells, and therefore, it directly controls the number of Type I cells and astrocytes in the population. The changes in θ were expected to affect all type of cells in the population, with a greater impact on Type I cell and astrocyte populations. Similar to α, this range of effect makes θ also one of the most critical parameters. For all cell types except neuroblasts, the population diminished until day 30 if $\theta < 0.5$, meaning that the model requires at least half of the Type I cell population to divide symetrically for populations to survive for 30 days (Figure 5). When all Type I cells divided symetrically, the number of astrocytes continued to exponentially increase as they are generated also from Type II cells and they can proliferate to renew their population. However, this increase reached to a plateau at $\theta = 0.9$, as Type I contribution almost completely disappears.

The rate τ_1 determines the ratio of Type II cells that proliferate to produce new Type II cells. The Type II cells that divided twice were assumed to either differentiate or die. Increase in τ_1 had a direct impact on the growth of all cell populations except Type I as expected. This effect was only observed for astrocyte population and was more pronounced for the other populations when $\tau_1 \geq 0.8$. The rate τ_2, on the other hand, controls the ratio of differentiating Type II cells. The cells that did not divide at least once were assumed to lack the ability to differentiate. The amount of Type II cells decreased with increasing τ_2, as the number of cell choosing to proliferate decreased. This decrease slowed and reached to a plateau around $\tau_2 = 0.6$. It can be suggested that high τ_2 prevent replenishing the Type II cell pool, and creates a limit for the population

growth for the cell types except Type I cells, which are not affected by the changes in Type II cell population.

The default HANG model assumes that the neurogenic processes are not affected by aging. However, several studies reported the decrease in neurogenic capacity, especially in hippocampus, by aging [36], [37] due to a combined effect of several factors on neurogenic processes such as telomere shortening [38]. The impact of aging on adult hippocampal neurogenesis was recently addressed in a study that utilized a different framework of cell populations and neurogenic processes [35]. The HANG model produces similar age-implemented growth patterns of NSCs with this model and further proposes a pattern of growth for all cell types of HANG model. However, the HANG model should be developed further to include a realistic measure of environmental changes by age, not just predefined age borders to guide the system. The most active period of HANG and the rate of decline might change among species, which is yet another factor that should be taken into account.

The presented numerical model of SGZ-ANG with the implementation of *choice of fate* was successful to represent the *in vivo* decline pattern of BrdU+ (proliferating) cells - which would include Type I, Type II and Type III cells of the model - by age [29] . Even though the model should be expanded to account for experimental data more accurately, it still presents an efficient and simple method to estimate the population size of neurogenic niche cells, together with the characterization of critical rates that could be expanded via including the effect of chemical and physical factors regulating SGZ-ANG. With or without these expansions, the numerical model can be implemented in a hippocampal network model to mimic the time-dependent production of newborn neurons at the dentate gyrus.

Acknowledgment

References

[1] Kempermann, G., Song, H., Gage, F. H. 2015. Neurogenesis in the adult hippocampus. Cold Spring Harbor Perspectives in Biology, 7(9), a018812.

[2] Kempermann, G. 2015. Adult neurogenesis: An evolutionary Perspective. Cold Spring Harbor Perspectives in Biology, 8(2), a018986.

[3] Morrens, J., Van Den Broeck, W., Kempermann G. 2012. Glial cells in adult neurogenesis. Glia, 60(2), 159-174.

[4] Ehninger, D., Kempermann, G. 2008. Neurogenesis in the adult hippocampus. Cell and Tissue Research, 331(1), 243-250.

[5] Amrein, I., Lipp, H. P. 2009. Adult hippocampal neurogenesis of mammals : evolution and life history. Biology Letters, 5, 141-144.

[6] Berg, D.A., Bond, A. M., Ming G., Song, H. 2018. Radial glial cells in the adult dentate gyrus: what are they and where do they come from? Cell and Tissue Research, 7, 277.

[7] Seri,B. , Garcia-Verdugo, J. M. , McEwen, B. S. , Alvarez-Buylla, A. 2001. Astrocytes give rise to new neurons in the adult mammalian hippocampus. Journal of Neuroscience, 21(18), 7153-7160.

[8] Kronenberg, G., Reuter, K., Steiner, B., Brandt, M. D., Jessberger, S., Yamaguchi, M., Kempermann, G. 2003. Subpopulations of proliferating cells of the adult hippocampus respond differently to physiologic neurogenic stimuli. Journal of Comparative Neurology, 467(4), 455-463.

[9] Gebara, E., Bonaguidi, M. A., Beckervordersandforth, R., Sultan, S., Udry, F., Gijs, P. J., Lie, D. C., Ming, G. L., Song, H., Toni, N. 2016. Heterogeneity of Radial Glia-Like Cells in the Adult Hippocampus. Stem Cells, 34(4), 997-1010.

[10] Amaral, D. G., Witter, M. P. 1989. The three-dimensional organization of the hippocampal formation: a review of anatomical data. Neuroscience, 31(3), 571-591.

[11] Jinno, S. 2011. Topographic differences in adult neurogenesis in the mouse hippocampus: a stereology-based study using endogenous markers. Hippocampus, 21(5), 467-480.

[12] Piatti, V. C., Davies-Sala, M. G., Esposito, M. S., Mongiat, L.A., Trinchero, M.F., Schinder, A.F. 2011. The timing for neuronal maturation in the adult hippocampus is modulated by local network activity. Journal of Neuroscience, 31(21), 997-1010.

[13] Jhaveri, D. J., O'Keeffe, I., Robinson, G. J., Zhao, Q. Y., Zhang, Z. H., Nink, V., Narayanan,R. K., Osborne, G.W., Wray, N. R., Bartlett, P.F. 2015. Purification of neural precursor cells reveals the presence of distinct, stimulus-specific subpopulations of quiescent precursors in the adult mouse hippocampus.Journal of Neuroscience, 35(21), 8132-8144.

[14] Hodge, R D., Kowalczyk, T.D., Wolf, S. A., Encinas, J. M., Rippey, C., Enikopolov, G., Kempermann, G., Hevner, R. F. 2008. Intermediate progenitors in adult hippocampal neurogenesis: Tbr2 expression and coordinate regulation of neuronal output. Journal of Neuroscience, 28(4), 3707-3717.

[15] Berg, D. A., Yoon, K., Will, B., Xiao, A.Y., Kim, N., Christian, K. M., Song, H., Ming, G. 2015. Tbr2-expressing intermediate progenitor cells in the adult mouse hippocampus are unipotent neuronal precursors with limited amplification capacity under homeostasis. Frontiers in Biology, 10(3), 262-271.

[16] Garcia, A. D., Doan, N. B., Imura, T., Bush, T. G., Sofroniew, M. V. 2004. GFAP-expressing progenitors are the principal source of constitutive neurogenesis in adult mouse forebrain. Nature Neuroscience, 7(11), 1233-1241.

[17] Suh, H., Consiglio, A., Ray, J., Sawai, T., D'Amour, K. A., Gage, F. H. 2007. In vivo fate analysis reveals the multipotent and self-renewal capacities of Sox2+ neural stem cells in the adult hippocampus. Cell Stem Cell, 1(5), 515-28.

[18] Huttner, W. B. 2015. Stem cells: slow and steady wins the race. Nature Neuroscience, 18, 613-614.

[19] Rusznak, Z., Henskens, W., Schofield, E., Kim, W. S., Fu, Y. 2016. Adult Neurogenesis and Gliogenesis: Possible Mechanisms for Neurorestoration. Experimental Neurobiology,25(3),103-112.

[20] Colak, D., Mori, T., Brill, M. S., Pfeifer, A., Falk, S., Deng, C., Monteiro, R., Mummery, C., Sommer, L., Götz, M. 2008. Adult neurogenesis requires Smad4-mediated bone morphogenic protein signaling in stem cells. Journal of Neuroscience, 28, 434-446.

[21] Hack, M. A., Sugimori, M., Lundberg, C., Nakafuku, M., Götz, M. 2004. Regionalization and fate specification in neurospheres: the role of Olig2 and Pax6. Molecular and Cellular Neuroscience,25,664–678.

[22] Doetsch, F., Petreanu, L., Caille, I., Garcia-Verdugo, J. M., Alvarez-Buylla, A. 2002. EGF converts transit-amplifying neurogenic precursors in the adult brain into multipotent stem cells. Neuron,36,1021–1034.

[23] Heins, N., Malatesta, P., Cecconi, F., Nakafuku, M., Tucker, K. L., Hack, M. A., Chapouton, P., Barde, Y. A.,G,tz, M. 2002. Glial cells generate neurons: the role of the transcription factor Pax6.Nature Neuroscience,5,308–315.

[24] Berninger, B., Costa, M. R., Koch, U., Schroeder, T., Sutor, B., Grothe, B., Götz, M. 2007. Functional properties of neurons derived from in vitro reprogrammed postnatal astroglia. Journal of Neuroscience,27,8654–8664.

[25] Heinrich, C., Blum, R., Gascón, S., Masserdotti, G., Tripathi, P., Sánchez, R., Tiedt, S., Schroeder, T, Götz M, Berninger B. 2010. Directing astroglia from the cerebral cortex into subtype specific functional neurons. PLoS Biology,8,e1000373.

[26] Niu, W., Zang, T., Zou, Y., Fang, S., Smith, D. K., Bachoo, R., Zhang, C. L. 2013. In vivo reprogramming of astrocytes to neuroblasts in the adult brain. Nature Cell Biology,15,1164–1175.

[27] Jackson, E. L., Garcia-Verdugo, J. M., Gil-Perotin, S., Roy, M., Quinones-Hinojosa, A., VandenBerg, S., Alvarez-Buylla, A. 2006. PDGFR alpha-positive B cells are neural stem cells in the adult SVZ that form glioma-like growths in response to increased PDGF signaling. Neuron,51,187–199.

[28] Goncalves, J. T., Schafer, S. T., Gage, F. H. 2016 Adult Neurogenesis in the Hippocampus: From Stem Cells to Behavior. Cell,167,897-914.

[29] Klempin, F., Beis, D., Mosienko, V., Kempermann, G., Bader, M., Alenina, N. 2013. Serotonin is required for exercise-induced adult hippocampal neurogenesis. Journal of Neuroscience, 33(19), 8270-8275.

[30] Lugert, S., Kremer, T., Jagasia, r., Herrmann, A., Aigner, S., Giachino, C., Mendez-David, I., Gardier, A.M., Carralot, J. P., Meistermann, H., Augustin, A., Saxe, M. D., Lamerz, J., Duran-Pacheco, G., Ducret, A., Taylor, V., David, D. J., Czech, C. 2017 Glypican-2 levels in cerebrospinal fluid predict the status of adult hippocampal neurogenesis. Scientific Reports, 7, 46543.

[31] Miller, J.A., Nathanson, J., Franjic, D., Shim, S., Dalley, R.A., Shapouri, S., Smith, K. A., Sunkin, S. M., Bernard, A., Bennett, J. L., Lee, C., Hawrylycz, M. J., Jones, A. R., Amaral, D. G., Sestan, N., Gage, F. H., Lein, E. S. 2013. Conserved molecular signatures of neurogenesis in the hippocampal subgranular zone of rodents and primates. Development, 140, 4633-4644.

[32] Ashbourn, J. M.iller, J., Reumers, V., Baekelandt, V., Geris, L. 2012. A mathematical model of adult subventricular neurogenesis. Journal of Royal Society,Interface, 9(75), 2414-2423.

[33] Ziebell, F., Martin-Villalba, A., Marciniak-Czohra, A. 2014. Mathematical modelling of adult hippocampal neurogenesis: effects of altered stem cell dynamics on cell counts and bromodeoxyuridine-labelled cells.

Journal of Royal Society,Interface, 11(94), 20140144.

[34] Choi, M.L., Begeti, F., Barker, R.A., Kim, N. 2015. A simple assessment model to quantifying the dynamic hippocampal neurogenic process in the adult mammalian brain. Hippocampus, 26(4), 517-529.

[35] Ziebell, F., Dehler, S., Martin-Villalba, A., Marciniak-Czohra, A. 2018. Revealing age-related changes of adult hippocampal neurogenesis using mathematical models. Development, 145(1), dev153544.

[36] Kuhn, H. G., Dickinson-Anson, H., Gage, F. H. 1996. Neurogenesis in the dentate gyrus of the adult rat: age-related decrease of neuronal progenitor proliferation. Journal of Neuroscience, 16(6), 2027-2033.

[37] Encinas, J. M., Michurina, T.V., Peunova, N., Park, J.H., Tordo, J., Peterson, D.A., Fishell, G., Koulakov, A., Enikopolov, G. 2011. Division-coupled astrocytic differentiation and age-related depletion of neural stem cells in the adult hippocampus. Cell Stem Cell, 8(5), 566-579.

[38] Rolyan, H., Scheffold, A., Heinrich, A., Begus-Nahrmann, Y., Langkopf, B.H., Hölter, S.M., Vogt-Weisenhorn,D. M., Liss, B., Wurst, W., Lie,D. C., Thal, D. R., Biber, K., Rudolph, K. L. 2011. Telomere shortening reduces Alzheimer's disease amyloid pathology in mice. Brain, 134(7), 2044-2056.